The Net Orientation of Nicotinic Receptor Transmembrane α-Helices in the Resting and Desensitized States

Danny G. Hill and John E. Baenziger

Department of Biochemistry, Microbiology, and Immunology, University of Ottawa, Ottawa, Ontario, Canada

ABSTRACT The net orientation of nicotinic acetylcholine receptor transmembrane α-helices has been probed in both the activatable resting and nonactivatable desensitized states using linear dichroism Fourier-transform infrared spectroscopy. Infrared spectra recorded from reconstituted nicotinic acetylcholine receptor membranes after 72 h exposure to ^2H_2O exhibit an intense amide I component band near 1655 cm^{-1} that is due predominantly to hydrogen-exchange-resistant transmembrane peptides in an α-helical conformation. The measured dichroism of this band is 2.37, suggesting a net tilt of the transmembrane α-helices of roughly 40° from the bilayer normal, although this value overestimates the tilt angle because the measured dichroism at 1655 cm^{-1} also reflects the dichroism of overlapping amide I component bands. Significantly, no change in the net orientation of the transmembrane α-helices is observed upon agonist binding. In fact, the main changes in structure and orientation detected upon desensitization involve highly solvent accessible regions of the polypeptide backbone. Our data are consistent with a capping of the ligand binding site by the solvent accessible C-loop with little change in the structure of the transmembrane domain in the desensitized state. Changes in structure at the interface between the ligand-binding and transmembrane domains may uncouple binding from gating.

INTRODUCTION

The nicotinic acetylcholine receptor (nAChR) from *Torpedo* is the best characterized member of a superfamily of structurally related neurotransmitter-gated ion channels (1–3). These neurotransmitter receptors mediate the transfer of chemical information between neurons in both the central and peripheral nervous systems as well as at the neuromuscular junction. The nAChR is composed of four subunits organized pseudosymmetrically as an $\alpha_2\beta\gamma\delta$ pentamer around a central ion channel pore. Each of the four subunits contains a large extramembranous domain, four hydrophobic membrane-spanning segments, M_1 to M_4, and a cytoplasmic loop between the M_3 and M_4 transmembrane segments. The M_2 transmembrane segment from each subunit shapes the lumen of the channel pore, and forms the gate of the closed channel.

With the solution of the three-dimensional structure of the acetylcholine binding protein—a snail glial protein with significant homology to the extracellular domain of the nAChR (4,5)—increasing attention has focused on the structure of the nAChR and its transmembrane domain, as well as the nature of nAChR conformational change. Although initial structural studies suggested the existence of transmembrane β-strands (6,7), considerable biochemical and structural data confirm an essentially α-helical transmembrane domain structure (8–16). Channel gating appears to result from a slight twist of the pore-lining M2 transmembrane α-helices (17). Changes in structure of the ligand-binding domain upon agonist binding have been identified (4,5,18). In light of recent models of nAChR structure, the roles of residues along the gating pathway between the binding site and the transmembrane domains have also been tested (19–22). Less work has focused on identifying the structural changes associated with formation of the channel inactivatable desensitized state.

Fourier transform infrared (FTIR) spectroscopy has been used extensively to examine the structure of the nAChR and other integral membrane proteins. Our early FTIR studies showed that the nAChR is a mixed α-helical/β-sheet protein with an α-helical transmembrane domain (11–13). The latter conclusion was based on the strong α-helical character of the amide I band observed in FTIR spectra of nicotinic receptors treated with proteinase K to remove the extramembranous domains. In addition, 20–30% of the nAChR peptide hydrogens were found to be resistant to hydrogen-deuterium exchange, even after 72 h exposure to ^2H_2O at 4°C. These exchange-resistant peptides exhibit a strong amide I component band near 1655 cm^{-1} that is characteristic of α-helical structures. As peptides located in the transmembrane domain likely comprise a substantial proportion of the exchange-resistant core, the spectroscopic data suggest that the transmembrane domain of the nAChR has an α-helical structure.

The ability to isolate features in the infrared spectrum of the nAChR that are due predominantly to exchange-resistant peptides located within the transmembrane domain provides a means for probing structural features of this domain under a variety of conditions, such as in the ligand-bound and ligand-free state. In this report, we probe the orientational properties of the hydrogen-deuterium exchange-resistant core of the intact nAChR using linear dichroism attenuated total reflectance (ATR) infrared spectroscopy. Our results confirm that

Submitted February 3, 2006, and accepted for publication April 20, 2006.

Address reprint requests to John E. Baenziger, Dept. of Biochemistry, Microbiology, and Immunology, University of Ottawa, 451 Smyth Rd., Ottawa, ON, Canada, K1H 8M5. Tel.: 613-562-5800 ext. 8222; Fax: 613-562-5440; E-mail: jebaenz@uottawa.ca.

0006-3495/06/07/705/10 $2.00

doi: 10.1529/biophysj.106.082693

the nAChR transmembrane domain is composed of α-helices that are preferentially oriented parallel to the bilayer normal. No net change in the orientation of these exchange-resistant α-helices is detected upon carbamylcholine (Carb) binding. In fact, the most intense vibrational intensity changes detected upon desensitization are due to a change in conformation and orientation of highly solvent-exposed regions of the peptide backbone. Our results are consistent with the hypothesis that the main structural change that occurs in the nAChR upon desensitization involves closing of the C-loop around the ligand to form a high-affinity ligand-bound state.

EXPERIMENTAL PROCEDURES

Sample preparation

The nAChR from frozen *Torpedo californica* electric tissue (Aquatic Research Consultants; San Pedro, CA) was affinity purified and reconstituted into membranes composed of 1-palmitoyl-2-oleoyl-*sn*-glycero-3-phosphocholine/1-palmitoyl-2-oleoyl-*sn*-glycero-3-phosphate/cholesterol (PC/PA/Chol) 3:1:1 (mol/mol/mol) as described elsewhere (23). Aliquots of reconstituted nAChR membrane protein (250 μg) were then centrifuged, resuspended in 2 mM phosphate ^2H_2O buffer (pH 7.8), and left at 4°C to exchange peptide N-^{1}H with N-^{2}H. After 72 h exposure to ^2H_2O, the samples were frozen at −80°C until use.

nAChR membrane films were prepared for FTIR spectroscopy by slowly drying a 50-μl aliquot of the nAChR containing 250 μg of protein on the surface of a 50 × 20 × 2-mm germanium internal reflection element (IRE) under a gentle stream of N_2 gas. Alternatively, pure lipid membrane films of PC/PA/Chol 3:1:1 (mol/mol/mol) were prepared by slowly evaporating a solution containing all three lipids in chloroform (300 μg total of lipid) on the IRE surface. Both reconstituted and pure membrane lipid films thus deposited on the germanium IREs were placed inside a vertical ATR sample holder (Harrick, Ossining, NY) and were immediately hydrated with ^2H_2O *Torpedo* Ringer buffer (5 mM Tris, 250 mM NaCl, 5 mM KCl, 3 mM $CaCl_2$, and 2 mM $MgCl_2$, pH 7).

Polarized FTIR measurements

FTIR spectra were recorded using the ATR technique on a Digilab FTS-575 spectrometer (Randolf, MA) equipped with a DTGS detector. Linear dichroism spectra were obtained using a computer-controlled ZnSe polarizer from Pike Technologies (Madison, WI). All spectra were derived from 256 single beam scans taken at 2 cm^{-1} resolution, except for the spectra of nAChR-membrane films used for deconvolution (see Fig. 4), which were derived from 4000 single beam scans. The polarized single-beam spectra were ratioed against a corresponding background recorded using polarized light. Polarized spectra of the pure lipid films were recorded at 3°C intervals as the sample was cooled from 25°C to −15°C using a circulating water bath from Neslab. A 30-min time interval was allowed at each temperature for sample equilibration. All data processing was performed on GRAMS/AI 7.02 (Thermo Galactic, Salem, NH). Spectra were deconvolved using a gamma factor of 7 and a smoothing of 80% (24).

FTIR difference spectra

FTIR difference spectra were recorded as described in detail elsewhere (23,25). Briefly, spectra of nAChR membranes deposited on the surface of a germanium IRE were recorded while flowing *Torpedo* Ringer buffer past the film surface. Two predominantly resting-state spectra were recorded in the absence of Carb (512 scans each, 8 cm^{-1} resolution). The buffer was then switched to an identical flowing buffer containing 50 μM Carb and a spectrum was recorded of the desensitized state. The differences between the two resting-state spectra (control difference spectrum) and between the desensitized and second resting-state spectrum (Carb difference spectrum) were calculated and stored. The nAChR film was then washed with buffer for 20 min to remove Carb from the membrane film and the process was repeated many times. Difference spectra were obtained from a minimum of two different membrane films and were recorded either with or without the polarization accessory. For the polarized Carb-difference spectra, spectral differences were alternately recorded with the light polarized either parallel or perpendicular to the plain of incidence.

Calculation of order parameters for thick membrane films

The dichroic ratio, R, is defined as the ratio of the absorption intensities of a vibration observed with the incident infrared radiation polarized parallel versus perpendicular to the plane of incidence with the IRE:

$$R = \frac{A_{II}}{A_{\perp}}. \tag{1}$$

As described by Hübner and Mantsch (26; see also Goormaghtigh and Ruysschaert (27)) for experimental conditions the same as those used here (45° angle of incidence, thick film approximation, refractive index for the lipid film, $n_2 = 1.44$, and for the germanium IRE, $n_1 = 4$), the dichroic ratio R for the methylene symmetric CH stretching vibration (~2850 cm^{-1}) can be interpreted in terms of the order parameter that we refer to as S_{CH}:

$$S_{CH} = -2\frac{R-2}{R+1.45}. \tag{2}$$

S_{CH} is defined by the composite angle between all methylene symmetric C-H transition dipoles and the normal to the germanium IRE surface (26). We assume that the transition dipole lies in the methylene H-C-H plane and, in the all-*trans* configuration, is perpendicular to the long axis of the acyl chain. The absolute value of S_{CH} ranges from 1 ($R = 0.85$) for a film composed of lipids with all-*trans* saturated acyl chains uniformly oriented normal to the surface of the germanium IRE, to a value of 0 ($R = R_{ISO} = 2$) for a completely disordered system (26). Disorder leading to a concomitant decrease in the value of S_{CH} can result from 1), a deviation of the orientation of individual methylene segments relative to the acyl chain long axis, as occurs with local molecular motions (*trans-gauche* isomerization) and with methylene carbons adjacent to a double bond; and 2), an increase in the nonuniformity or mosaic spread of the membrane film on the IRE surface. We describe these two effects using the order parameters $S_{\text{acyl chain}}$ (S_{AC}) and $S_{\text{mosaic spread}}$ (S_{MS}), respectively, which are related to S_{CH} by the following equation:

$$S_{CH} = S_{AC}S_{MS}. \tag{3}$$

Calculation of α-helix orientation

The dichroic ratio for the amide I vibration can be interpreted in terms of what we refer to as the amide I order parameter, S_{AI}:

$$S_{AI} = \frac{R-2}{R+1.45}. \tag{4}$$

In this interpretation, S_{AI} is defined by the composite angle between a transition dipole that has an average orientation parallel to the long axis of the molecule (as opposed to S_{CH}, where the transition dipole is perpendicular) (26). As the amide I transition dipole is not oriented parallel to the long axis of an α-helix, we must take into account additional geometric terms (27,28), as follows:

$$S_{AI} = S_H S_G S_{MS}. \tag{5}$$

$S_H = (3Cos^2\theta - 1)/2$ defines the average angle, θ, between the α-helix long axis and the bilayer normal and $S_{geometry}$ (S_G) $= (3Cos^2\beta - 1)/2$ defines the average angle, β, between the amide I transition dipole and the long axis of the α-helix (we have used $\beta = 39°$ according to Bradbury et al. (29), Tsuboi (30), and Marsh et al. (31)). As in the previous case, the value of S_{AI} can be influenced by the mosaic spread of the membrane film. Note that a dichroic ratio $R = R_{ISO} = 2$ would correspond to an S_{A1} of 0, suggesting that the α-helix is either isotropically oriented relative to the bilayer normal to the germanium IRE or is tilted at the magic angle of 54.7° away from the bilayer normal. A dichroic ratio $R_{ISO} > 2$ suggests a predominant orientation parallel to the bilayer normal—i.e., a tilt angle away from the normal of <54.7°.

RESULTS AND DISCUSSIONS

The orientation of membrane protein functional groups relative to the membrane surface can be measured using linear dichroism FTIR spectra recorded from oriented membrane films deposited on the surface of a planar germanium internal reflection element (IRE). As discussed under Experimental Procedures, a rigorous mathematical interpretation of the linear dichroism data requires knowledge of the orientational uniformity or mosaic spread of these films on the IRE surface. We describe the mosaic spread by an order parameter, S_{MS}, which varies from 1 to 0 for membranes uniformly oriented parallel to and membranes randomly oriented on the IRE surface, respectively.

To estimate the extent of the mosaic spread in reconstituted nAChR membrane films, we recorded linear dichroism spectra from films formed from both pure lipid and reconstituted PC/PA/Chol 3:1:1 (mol/mol/mol) membranes, and compared the dichroism of several lipid vibrations (see below). We expected the pure lipid membranes, which were deposited on the IRE from chloroform, to form a well-oriented film with relatively low mosaic spread. The pure membranes thus serve as a control for assessing the linear dichroism of lipid vibrations in a relatively well-oriented system. In contrast, the reconstituted nAChR membranes were deposited as vesicles from aqueous solution. In both cases, the samples were dried under N_2 and the membranes hydrated with excess *Torpedo* Ringer buffer. Note that PC/PA/Chol 3:1:1 membranes are particularly effective at stabilizing the nAChR in a functional resting state that fluxes cations upon agonist binding (32–34). We have shown previously that this method of film formation on a planar surface yields functional receptors (25).

The most useful lipid vibration for assessing the mosaic spread of the lipid membranes is the acyl chain methylene symmetric C-H stretching vibration centered near 2850 cm^{-1}. The dichroic ratio (R) of this vibration can be interpreted in terms of an order parameter that we refer to as S_{CH} (see Experimental Procedures). The value of S_{CH} is determined by the composite orientation of all methylene C-H segments relative to the normal to the germanium IRE surface and is thus influenced by motions of the acyl chain (*trans-gauche* isomerizations), distortions of methylene carbons from the all-*trans* configuration due to their locations adjacent to a double bond, etc., and by the mosaic spread of the membrane film on the IRE surface (see Experimental Procedures). The dichroic ratio for the C-H stretching vibration reaches a minimum of 0.85, corresponding to $S_{CH} = 1.0$, for perfectly ordered all-*trans* saturated chains oriented perpendicular to the bilayer surface in a membrane film with no mosaic spread. Conversely, the dichroic ratio for this vibration can increase to a maximal value of 2.0, which corresponds to the dichroic ratio (R_{iso}) of an isotropically oriented sample. $R_{iso} = 2$ corresponds to $S_{CH} = 0$. An increase in the measured dichroic ratio of C-H stretching vibration could reflect an increasing deviation of the average orientation of the methylene segments away from the all-*trans* configuration, as occurs with increasing acyl chain motion or increasing film mosaic spread. Note that all perpendicularly polarized infrared spectra presented here have been multiplied by R_{ISO} to facilitate comparison with the corresponding parallel polarized spectra. After scaling, an absorbance intensity in a parallel polarized spectrum that is greater than the corresponding absorbance intensity in the perpendicular polarized spectrum signifies a net orientational preference parallel to the bilayer normal.

The methylene symmetric stretching vibration is also of interest because it undergoes a shift up in frequency with increasing acyl chain disorder (i.e., increasing methylene *trans-gauche* isomerizations). The C-H stretching frequency provides a sensitive probe of the transition from the ordered gel phase to the relatively disordered liquid crystalline phase. Previous studies have shown that incorporation of the nAChR into PC/PA/Chol 3:1:1 leads to a shift in the gel-to-liquid-crystal phase transition temperature from ~4°C up to ~13°C (23).

The lipid ester carbonyl stretching vibrations centered near ~1750 cm^{-1} are of interest in the discussion presented here. This band is composed of two underlying components centered near 1740 and 1730 cm^{-1} that reflect non-hydrogen-bonded and hydrogen-bonded lipid ester carbonyls, respectively. A membrane with a tighter lateral packing has less water penetration into the bilayer interfacial region and, thus, a greater proportion of non-hydrogen-bonded ester carbonyls vibrating near 1740 cm^{-1}. For example, tightly packed gel-phase membranes composed of PC/PA/Chol 3:1:1 membranes exhibit a higher proportion of non-hydrogen-bonded ester carbonyls near 1740 cm^{-1} than is observed in the same membranes in the liquid crystalline phase (Fig. 1 *C*, *top* and *middle traces*). Incorporation of the nAChR into the PC/PA/Chol 3:1:1 membrane leads to an increase in the proportion of non-hydrogen-bonded lipid ester carbonyls, suggesting a lateral tightening of the lipid bilayer, as noted previously (23).

Linear dichroism spectra from membrane films composed of PC/PA/Chol 3:1:1

We first recorded linear dichroism FTIR spectra from PC/PA/Chol 3:1:1 membrane films lacking the nAChR, which

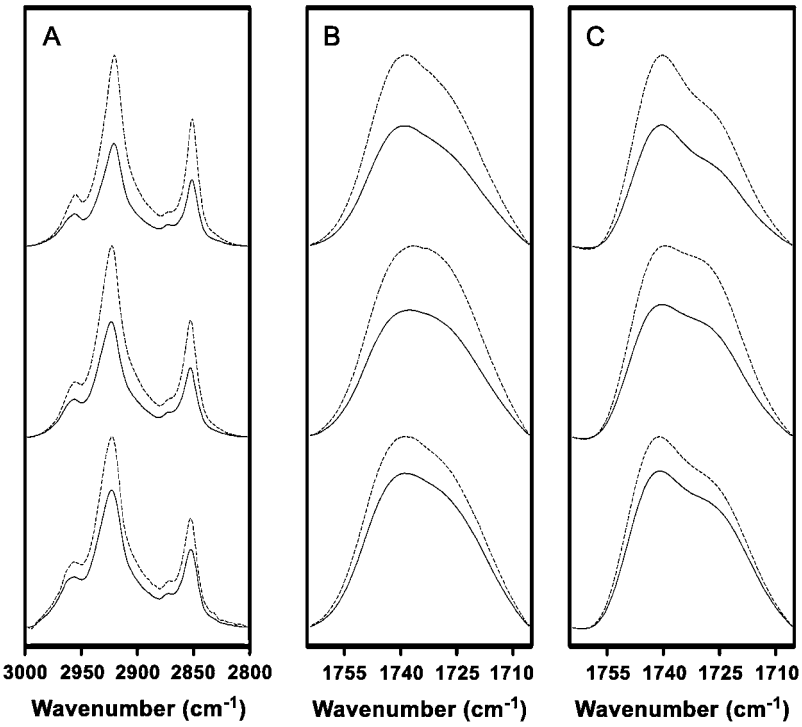

FIGURE 1 A comparison of polarized FTIR spectra of PC/PA/Chol 3:1:1 membranes collected at −5°C (*top traces*) and at 22.5°C (*middle traces*), as well as spectra of the reconstituted nAChR in PC/PA/Chol 3:1:1 membranes at 22.5°C (*bottom traces*). FTIR spectra of the membranes were recorded with either perpendicular polarized light (*dashed lines*) or parallel polarized light (*solid lines*). The spectra collected with perpendicular polarized light were multiplied by a factor of two to account for differences in the evanescent field strength (R_{ISO}). (*A*) Acyl chain C-H stretching bands. (*B*) Lipid ester carbonyl stretching band. (*C*) Deconvolved lipid ester carbonyl stretching band. Spectra were deconvolved between 1800 and 1600 cm^{-1} using gamma factor 10 and smoothing 80%.

we expected to be well-oriented on the IRE surface. Spectra recorded at 22.5°C exhibit a relatively high C-H stretching frequency near 2852 cm^{-1} and a relatively large proportion of hydrogen-bonded lipid ester carbonyls, as expected for a bilayer above its gel-to-liquid crystalline phase transition (compare Fig. 1, *A* and *B*, *top* and *middle traces*). At this temperature, the average dichroic ratio for the C-H symmetric stretching and the ester carbonyl stretching vibrations are 1.18 and 1.34, respectively, which compare well with the values of 1.3 and 1.4, respectively, obtained by Hübner and Mantsch for dipalmitoylphosphatidylcholine (DPPC) membrane films in the liquid crystalline phase (26). The dichroic ratio of the C-H stretching vibration corresponds to an order parameter, $S_{CH} = 0.63$, which is lower than the value expected for an ordered saturated chain in a membrane film with no mosaic spread. The low value of S_{CH} may reflect a substantial mosaic spread of the lipid film on the IRE surface. As noted, S_{CH} is sensitive to many factors, such as local acyl chain motions, that lead to deviations of the average methylene segment orientation away from the all-*trans* configuration. A decrease in S_{CH} will also occur with methylene segments located close to the unsaturated bond in the oleoyl chain.

To estimate the contributions of local acyl chain motions to both the observed dichroic ratio and the resulting order parameter, S_{CH}, we collected linear dichroism spectra from the PC/PA/Chol 3:1:1 membranes as the temperature was lowered from 22.5°C down to −15°C. As the PC/PA/Chol 3:1:1 membrane film is cooled below the gel-to-liquid crystalline phase transition (~4°C), the peak absorption frequency of the C-H stretching vibration decreases by roughly 2 cm^{-1} and the lipid ester carbonyl band changes shape in a manner indicative of an increase in the proportion of non-hydrogen-bonded lipid ester carbonyls (Fig. 1, *A* and *B*, *upper traces*). The latter reflects a lateral tightening of the lipid bilayer and a consequent decrease in the degree of water penetration into the bilayer interfacial region. Note that the phase transition of the PC/PA/Chol 3:1:1 bilayers from the liquid crystal to the gel phase is broader and appears to occur at a slightly higher temperature than observed in previous experiments performed using a transmission FTIR cell. The breadth of the transition may reflect an inability to control tightly the sample temperature in the ATR cell using a circulating water bath.

In the gel phase, the measured dichroic ratio for the acyl chain C-H symmetric stretching vibrations decreases from 1.18 to a value of 1.00, which corresponds to an order parameter $S_{CH} = 0.82$ (Fig. 2 and Table 1). The dichroic ratio is close to the value of 1.1 reported by Hübner and Mantsch for DPPC in the gel phase (26). An order parameter of $S_{CH} = 0.82$ is closer to the order parameter expected for a perfectly ordered saturated membrane with C-H transition dipoles oriented perpendicular to the bilayer normal. Our results show that the pure lipid films are highly ordered on the germanium IRE, and that mosaic spread contributes an order parameter of at most $S_{CH} = 0.82$ to S_{CH}. A value of 0.82 likely represents an overestimate of the contribution of mosaic spread to S_{CH}, as the presence of unsaturation in the PC and PA lipids will also contribute to a drop in S_{CH} (see above). The similarity of the dichroic ratios obtained for our unsaturated PC/PA/Chol membranes and saturated DPPC lipids

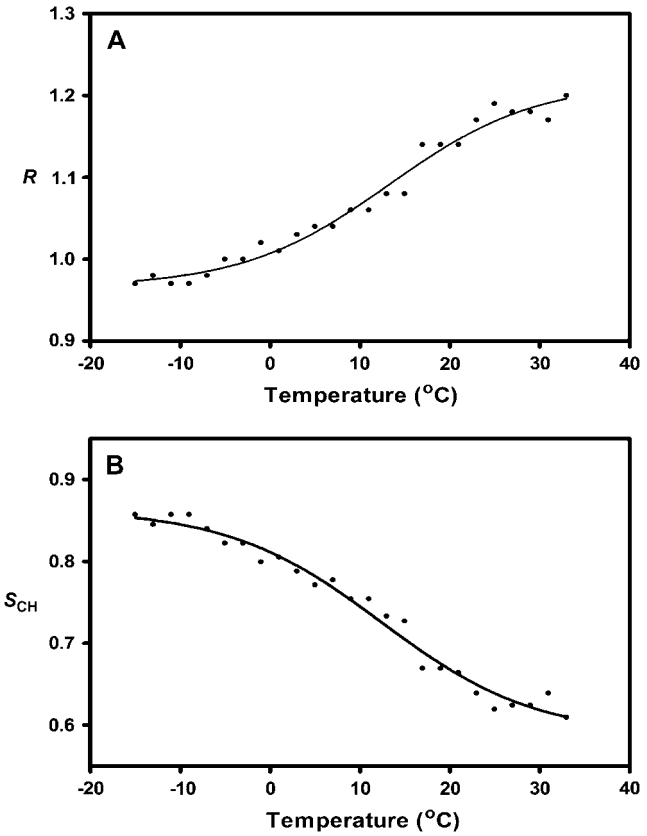

FIGURE 2 The dependence of the PC/PA/Chol 3:1:1 membrane acyl chain C-H symmetric stretching vibration dichroic ratio (*A*) and order parameter (*B*) on temperature.

(26) may indicate that mosaic spread is the main contributor to the S_{CH} value of 0.82.

Linear dichroism spectra from reconstituted nAChR membrane films

Linear dichroism spectra were next recorded from reconstituted nAChR membranes, and the dichroic ratios of the lipid vibrations were compared to those observed for the ''well-oriented'' pure lipid bilayer films (Table 1). At room temperature, the dichroic ratio for the C-H symmetric stretching vibration in the reconstituted PC/PA/Chol 3:1:1 membranes is 1.30, which is comparable to values observed for lipids in other reconstituted membranes (linear dichroism ATR-FTIR spectra collected from rhodopsin gave a dichroic ratio of 1.34 (35)), but higher than that observed for the pure PC/PA/Chol 3:1:1 membranes. A dichroic ratio of 1.30 corresponds to an order parameter $S_{CH} = 0.51$.

In the gel phase, the dichroic ratio of the C-H stretching vibration in the reconstituted membranes drops from 1.34 to 1.15, which corresponds to a molecular order parameter of 0.66. As in the case of the liquid crystalline bilayers, the value of S_{CH} obtained for the reconstituted membranes in the gel phase is greater than the value of S_{CH} obtained for the pure PC/PA/Chol 3:1:1 membrane films.

The difference in order parameters observed for the lipid in the pure versus reconstituted PC/PA/Chol 3:1:1 membranes could reflect either an increase in the mosaic spread of the reconstituted bilayer films or an increase in the disorder of the fatty acyl chains in the presence of the nAChR (see Gonen et al. (36)), or a combination of both. Although the dichroic ratios do not allow us to distinguish between the two possibilities, previous studies have shown that incorporation of the nAChR into bilayers, such as PC/PA/Chol 3:1:1, which contain the anionic lipid PA leads to a lateral tightening of the bilayer and an increase in the gel-to-liquid crystalline phase transition (23). Indeed, the carbonyl stretching vibrations recorded here show that incorporation of the nAChR into the PC/PA/Chol 3:1:1 membranes leads to an increase in non-hydrogen-bonded ester carbonyls likely due to a lateral tightening of the lipid bilayer (Fig. 1 *C*, *bottom* versus *middle traces*). A lateral tightening of the bilayer should increase—not decrease—the acyl chain order of the bulk lipid. The increased dichroic ratio of the C-H stretching vibration and consequent decrease in molecular order parameter of the acyl chain in the presence of the nAChR may be due primarily to an increased mosaic spread of the reconstituted nAChR membranes relative to the pure lipid bilayers. A slight increase in mosaic spread is not surprising, given that the reconstituted membrane films were prepared from aqueous dispersions of lipid vesicles, as compared with the pure lipid films, which were prepared after drying lipids from chloroform on the IRE surface. In addition, the nAChR extends beyond the surface

TABLE 1 Dichroic ratios and order parameters for PC/PA/Chol 3:1:1 membranes and reconstituted nAChR in PC/PA/Chol 3:1:1 membranes

−nAChR	−5°C			22.5°C		
Assignment	Wavenumber (cm^{-1})	R_{ATR}	S_{CH}	Wavenumber (cm^{-1})	R_{ATR}	S_{CH}
ν $CH_{2\ sym}$	2852	1.00	0.82	2853	1.18	0.63
ν C=O	1733	1.27	—	1732	1.34	—
+ nAChR	−5°C			22.5°C		
Assignment	Wavenumber (cm^{-1})	R_{ATR}	S	Wavenumber (cm^{-1})	R_{ATR}	S_{CH}
ν $CH_{2\ sym}$	2852	1.15	0.66	2853	1.30	0.51
ν C=O	1733	1.33	—	1732	1.45	—

of the bilayer (2,15,16), which may influence the uniformity of packing of the lipid bilayers in the film and, thus, the mosaic spread.

Based on the above data, it is possible to calculate approximate limits for the contribution of mosaic spread to the order parameters obtained for the reconstituted lipid membrane films. If the deviation in the molecular order parameter, S_{CH}, from the theoretical value of 1 down to the observed value of 0.66 for the reconstituted membranes in the gel phase is due entirely to mosaic spread of the membranes on the germanium surface, then we can calculate a maximal mosaic spread corresponding to $S_{MS} = 0.66$. Alternatively, if we assume that the films formed using the lipid alone exhibit no mosaic spread (i.e., are perfectly oriented parallel to the IRE surface), then we can assign the drop in S_{CH} from 1.0 to 0.82 in the pure lipid bilayers to the structural distortion of some of the methylene segments away from the all-*trans* orientation perpendicular to the bilayer surface as a result of acyl chain unsaturation, etc. As a similar structural perturbation due to the unsaturated bond on the oleoyl chain would likely occur in the reconstituted nAChR membranes, we can assume that these acyl chain distortions contribute a factor of 0.82 (S_{AC}) to the drop in S_{CH}. We can then calculate the contribution of mosaic spread to the S_{CH} for the reconstituted membranes as $S_{MS} = S_{CH}/S_{AC} = 0.66/0.82$ (see Eq. 3 in Experimental Procedures). The minimal mosaic spread for the reconstituted membrane film is thus $S_{MS} = 0.80$. The true mosaic spread of the reconstituted membrane films likely lies somewhere between these two limits, i.e., $0.66 < S_{MS} < 0.80$.

Orientation of the nAChR transmembrane domain

Infrared spectra recorded from the reconstituted nAChR membranes exhibit two main protein bands that are sensitive to the secondary structure of the nAChR and can be analyzed in linear dichroism spectra to provide insight into the orientation of the nAChR transmembrane α-helical segments. The amide I vibration (1600–1700 cm^{-1}) is due mainly to peptide C=O stretching and is sensitive to hydrogen bonding and, thus, protein secondary structure. The amide II vibration (1620–1580 cm^{-1}) is due mainly to peptide N-^{1}H bending. This vibration shifts down in frequency to near 1450 cm^{-1} upon the exchange of peptide N-^{1}H for N-^{2}H. The residual amide II vibration intensity in spectra of the nAChR recorded in ^2H_2O reflects the number of peptide hydrogens that remain in the protiated form (11,37).

After 72 h exposure of the nAChR to ^2H_2O at 4°C, the amide I band shape is relatively broad and symmetric, with a maximum around 1640 cm^{-1} (37). Resolution enhancement shows that this broad band is composed of two main peaks centered near 1655 and 1630 cm^{-1} due to peptides in α-helical and β-sheet secondary structures, respectively, consistent with current models that predict a mixed α-helix/β-sheet structure for the nAChR (15,16). The residual amide II band intensity indicates that ~25% of the peptide hydrogens remain unexchanged for deuterium after 72 h in ^2H_2O (37). Further exchange of these exchange-resistant peptide hydrogens for deuterium under conditions, such as alkaline pH and increased temperature, that enhance peptide hydrogen-deuterium exchange leads to a downshift in frequency of the 1655-cm^{-1} amide I component band, suggesting that the 1655 cm^{-1} corresponds to exchange-resistant α-helical peptides (11). Given that ~75% of the α-helical peptides in the nAChR structure defined to date are part of the transmembrane domain (16), and that a strong correlation has been shown to exist between the percentage of exchange-resistant peptide hydrogens and the size of an integral membrane protein's transmembrane domain (see Baenziger and Méthot (37)), we conclude that the 1655 cm^{-1} α-helical amide I component band in the nAChR is due primarily to α-helical transmembrane peptides. Note that peptides in loop/random structures also vibrate near 1655 cm^{-1} in spectra of the nAChR recorded in ^1H_2O, but these vibrations shift down in frequency to near 1640 cm^{-1} immediately after exposure of the nAChR to ^2H_2O (38).

We probed the orientation of this exchange-resistant ''core'' of α-helices by recording linear dichroism spectra of the nAChR after 72 h exposure to ^2H_2O at 4°C. In an α-helical peptide, the amide I and amide II transition dipoles are preferentially oriented parallel and perpendicular, respectively, to the long axis of the α-helix. An α-helix with a net preferential orientation parallel to the bilayer normal will give rise to a dichroic ratio >2.0 for the amide I vibration and a dichroic ratio <2.0 for the amide II band. In contrast, an α-helix with a net orientation parallel to the bilayer surface will exhibit the opposite dichroism for the two vibrations—a dichroic ratio <2.0 for the amide I band and >2.0 for the amide II vibration. A randomly oriented α-helix should exhibit a dichroic ratio of $R_{ISO} = 2.0$ for both bands.

The linear dichroism spectra clearly show that the α-helical peptides in the exchange-resistant core of the nAChR exhibit a preferential orientation parallel to the bilayer normal as the dichroism of the amide I and the residual amide II band are >2.0 and <2.0, respectively (Fig. 3). We estimate the α-helical amide I component band dichroism near 1655 cm^{-1} to be 2.37. This corresponds to an average tilt of the transmembrane α-helices relative to the bilayer normal of either 40° or 43°, depending on whether we incorporate an S_{MS} value of 0.66 or 0.82 for the mosaic spread, respectively, into our calculations (see above). Our results suggest that mosaic spread does not make a large difference to the calculated net orientation of the nAChR transmembrane α-helices relative to the bilayer normal.

The average net tilt is higher than expected based on current models of nAChR structure, which indicate a net tilt of the transmembrane α-helices of 20° or less from the bilayer normal (15,16). Our data could suggest that the transmembrane α-helices are tilted away from the bilayer normal to a greater extent than in these models. The higher

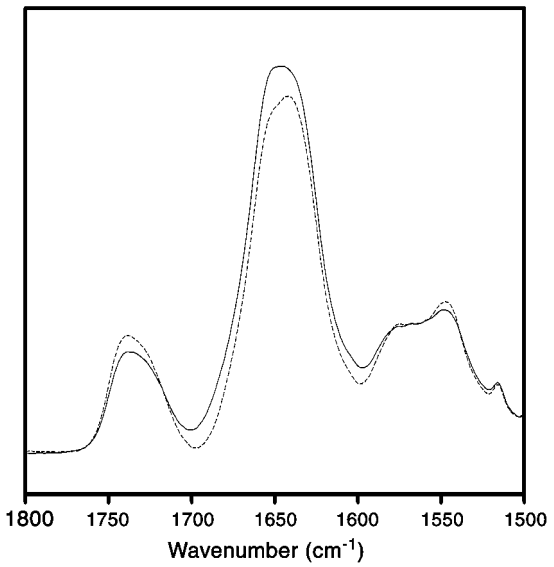

FIGURE 3 Polarized FTIR spectra of reconstituted nAChR PC/PA/Chol 3:1:1 membrane films. FTIR spectra collected at 22.5°C with perpendicular polarized light (*dashed lines*) and parallel polarized light (*solid lines*) are illustrated. The FTIR spectra recorded with perpendicular polarized light were multiplied by a factor of 2 to account for differences in the evanescent field strength (R_{ISO}).

tilt angle, however, could also reflect the fact that the broad α-helical amide I component band near 1655 cm^{-1} assigned to exchange-resistant α-helical structures overlaps with other broad amide I component bands due to β-sheet, random structures, and peptide hydrogen-exchanged α-helices. For example, the α1 helix at the periphery of the ligand-binding domain is tilted at an angle of ~65° from the bilayer normal (16). The dichroism of this and other bands lowers the measured dichroism at 1655 cm^{-1} and increases the calculated net tilt attributed to the transmembrane α-helical structures. The calculated net tilt of 40° relative to the bilayer normal for the transmembrane α-helices therefore represents an overestimation of the tilt angle.

Average tilt of transmembrane α-helices in the presence of Carb

Although a precise mathematical value for the average net tilt of the transmembrane α-helices is difficult to obtain due to the discussed band overlap, net changes in tilt angle of the transmembrane α-helices upon Carb binding should lead to measurable changes in dichroic ratio that can be accurately detected using FTIR spectroscopy (see below). The effect of desensitization on the net orientation of the transmembrane α-helices was determined by recording linear dichroism spectra in the presence and absence of the agonist Carb. To minimize sample-to-sample variations, the linear dichroism spectra in the presence and absence of Carb were both recorded from the same nAChR membrane film by exchanging the buffer surrounding the film in the ATR sample compartment. In the absence of Carb, the nAChR in PC/PA/Chol 3:1:1 adopts predominantly a low-affinity acetylcholine-binding resting conformation (32–34). After prolonged exposure to Carb, the nAChR adopts a relatively high-affinity acetylcholine-binding desensitized state. The linear dichroism spectra recorded from the nAChR in the presence of Carb are virtually identical to those recorded in its absence. This finding suggests that there is no net change in transmembrane α-helix orientation upon desensitization (Fig. 4).

To provide an estimate of the sensitivity of the FTIR linear dichroism measurements, we calculated the change in dichroic ratio that would result from a hypothetical 5° change in average orientation of all the exchange-resistant α-helices. A change in net orientation from 40° to 35° relative to the bilayer normal upon Carb binding would result in a change in dichroic ratio of the α-helical amide I band from 2.37 to 2.54 (assuming $S_{MS} = 0.66$). If we were to keep the parallel polarized absorption band intensity at 1655 cm^{-1} constant, a hypothetical change in dichroic ratio from 2.37 to 2.54 would require a change in intensity of the perpendicular polarized infrared absorption at 1655 cm^{-1} of ~5%. Such a change in intensity is easy to detect when the dichroic spectra are recorded in the presence and absence of Carb from the same nAChR film deposited on the ATR surface. A hypothetical change in orientation of only one of the four transmembrane α-helices (for example, M2) from each subunit by 5% would require a change in intensity of the perpendicular polarized band at 1655 cm^{-1} of only ~1%, which is close to the detection limit that one can observe using absorbance

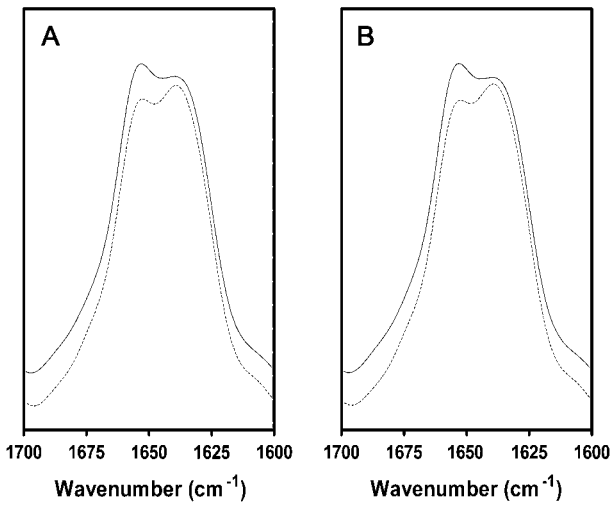

FIGURE 4 Deconvolved polarized FTIR spectra of reconstituted nAChR PC/PA/Chol 3:1:1 membrane films recorded in the absence (*A*) and presence (*B*) of 1 mM Carb. Deconvolved FTIR spectra collected with perpendicular polarized light (*dashed lines*) were multiplied by a factor of two (R_{ISO}) to account for differences in the evanescent field strength. FTIR spectra collected with parallel polarized light are illustrated by the solid lines. All four spectra were recorded sequentially from the same nAChR film.

measurements. These calculations show that the nAChR must only undergo subtle (only a few degrees) if any net change in the orientations of transmembrane α-helices upon agonist binding and desensitization.

Changes in orientation of the polypeptide backbone upon desensitization

Changes in orientation of peptide backbone upon desensitization were probed further by recording linear dichroism infrared difference spectra. In contrast to the data presented above (Fig. 4), where the orientation of *all* peptide bonds are probed in the resting and desensitized states, the difference between spectra repetitively recorded while flowing buffer either with or without the agonist Carb (a Carb-difference spectrum) past the nAChR film surface only exhibits vibrational bands from those regions of the protein that undergo the resting to desensitized conformational change. Specifically, a pattern of positive and negative vibrations is observed that results from 1), the appearance of vibrations from nAChR-bound Carb; 2), vibrational shifts reflecting the formation of physical interactions between Carb and residues in the nAChR binding site; and 3), vibrational shifts that reflect changes in structure of the peptide backbone upon transition from the resting to the desensitized state (39). Linear dichroism Carb-difference spectra can thus probe directly the changes in orientation of the peptide backbone that occur upon desensitization. Linear dichroism difference spectra can also shed light on the orientation of bound substrates (see below).

A Carb-difference spectrum recorded with unpolarized infrared light is presented in Fig. 5 *A* (*top trace*). This difference spectrum is the average of 62 individual difference spectra recorded from three separate days of data acquisition. The individual averages from each day are shown in the supplemental information to give a sense of the magnitude of the variations that are observed from one difference spectrum to the next. Note that the Carb difference spectrum exhibits two intense positive bands near 1655 and 1544 cm^{-1} that can be attributed to amide I and II vibrations, respectively, of the peptide backbone. These two bands appear as a result of the conformational change that occurs in the nAChR upon desensitization. The frequencies of both bands are characteristic of α-helical structures and thus could reflect a change in structure/orientation of transmembrane α-helices, although data discussed below suggest an alternative band assignment.

Carb-difference spectra recorded using either parallel or perpendicular polarized infrared light are presented in Fig. 5 *B* (*top* and *middle spectra*, respectively). The two difference spectra are the average of 79 and 77 individual difference spectra and the two are superimposed in the bottom trace of Fig. 5 *B* (see Supplemental Information for individual averages). There are subtle but reproducible variations in the intensities of several vibrations in the Carb-difference spectra recorded at the two polarizations (see Supplemental Information). Of particular interest here, the amide I vibration near 1655 cm^{-1} is less intense than the amide II vibration centered near 1544 cm^{-1} in the Carb-difference spectrum recorded using parallel polarized infrared light, whereas the relative intensities of the two vibrations are reversed in difference spectra recorded using perpendicular polarized infrared light.

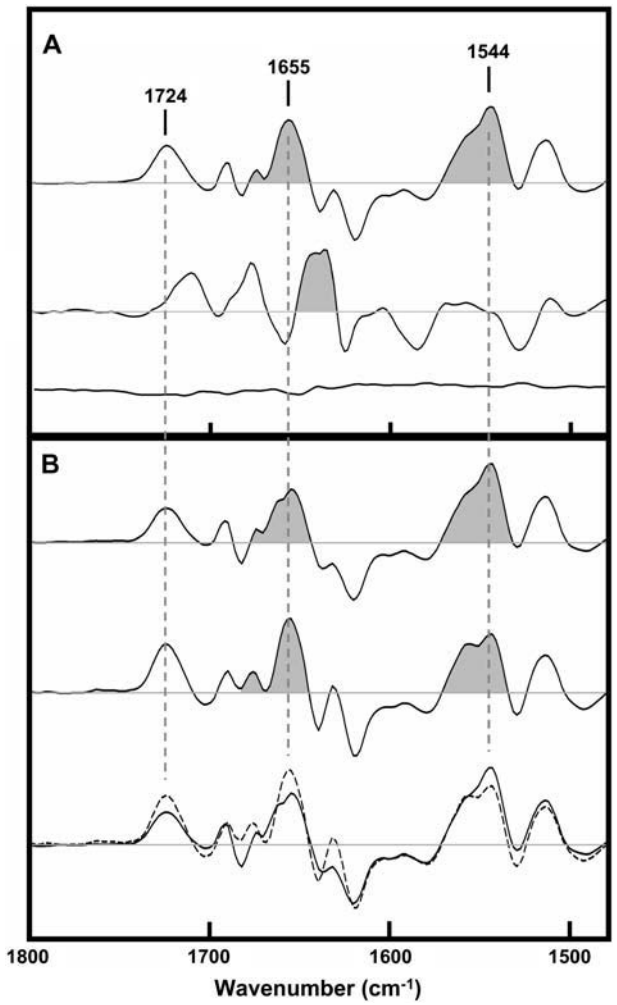

FIGURE 5 Carb-difference spectra recorded from the nAChR in PC/PA/Chol 3:1:1 membranes. (*A*) Carb-difference spectra recorded with unpolarized infrared light. The top trace was recorded in ^1H_2O buffer, whereas the middle trace was recorded in ^2H_2O buffer. The bottom trace is a control showing the difference between spectra both recorded in the absence of Carb. (*B*) Carb-difference spectra recorded with parallel (*top trace* and *solid line in bottom traces*) and perpendicular (*middle trace* and *dashed line in bottom traces*) polarized infrared light. The perpendicular polarized difference spectrum has been scaled to account for the difference in evanescent field strength (R_{ISO}).

If the amide I and II difference bands near 1655 and 1544 cm^{-1} were to reflect a change in orientation alone of the peptide backbone relative to the bilayer normal, one would expect a positive 1655-cm^{-1} band and a negative 1544-cm^{-1} band (or vice versa) in one of the linear dichroism difference spectra (i.e., either the parallel or the perpendicular polarized

difference spectrum, depending on the nature of the tilt) and the opposite intensities of the two bands in the other. Conversely, if the vibrations result from a change in conformation of the backbone alone, without any change in orientation, then the two vibrations should have identical relative intensities in both linear dichroism difference spectra. The fact that the 1655- and 1544-cm^{-1} bands exhibit positive intensity in both the parallel and perpendicular polarized difference spectra, but vary in terms of the ratios of their relative intensities, suggests that there is both a conformational change in the peptide backbone (leading to increased intensity of both amide bands) and a change in orientation of the backbone (leading to the altered ratios in intensity of the two peaks). The nature of the variations in amide I/II band intensity in the two linear dichroism difference spectra is consistent with a slight tilt of a transmembrane α-helix away from the bilayer normal in the desensitized state.

Note, however, that Carb-difference spectra previously recorded in ^2H_2O show that the amide I difference band centered near 1655 cm^{-1} undergoes a large downshift in frequency to near 1640 cm^{-1} upon exposure of the nAChR to ^2H_2O (Fig. 5 *A, middle trace*). In addition, this down shift in frequency is observed in difference spectra recorded after $<$10 min exposure of the nAChR to ^2H_2O (38). In contrast, vibrations due to α-helical secondary structures tend to undergo relatively small downshifts in frequency upon peptide hydrogen-deuterium exchange (38). The large and rapid downshift in frequency of the 1655 cm^{-1} band upon exposure of the nAChR to ^2H_2O thus suggests that the 1655 cm^{-1} vibration reflects a change in conformation and orientation of loop/random structures—not a change in orientation of the exchange-resistant transmembrane α-helices. In fact, there is no intensity observed in the difference spectra recorded in ^2H_2O that occurs at a frequency consistent with that of the unexchanged α-helical peptides observed in FTIR spectra in the nAChR. The changes in conformation/orientation of the peptide backbone detected here upon desensitization thus involve highly solvent accessible regions of the polypeptide backbone. Although we cannot rule out the possibility that pore-lining transmembrane α-helices exchange their peptide hydrogens rapidly with solvent, a more likely interpretation is that we are detecting a change in conformation/orientation of the solvent-accessible C-loop, which lines one surface of the ligand-binding site (16).

It is important to note that the magnitude of the changes in intensity observed in the linear dichroism difference spectra at 1655 cm^{-1} that we tentatively attribute to a change in orientation of loop structures are 50-fold less intense than the intensity change that would result from the hypothetical 5° changes in orientation of all four transmembrane α-helices of each subunit discussed above. The linear dichroism difference spectra should be sensitive enough to detect a tilt in a single transmembrane α-helix by only a few degrees. Our data suggest that there are minimal structural changes that occur in the transmembrane domain upon desensitization. Given that channel gating results from only a slight twisting of the pore-lining M2 transmembrane α-helix to remove bulky nonpolar side chains from the channel lumen (17), it is not surprising that desensitization, which does not lead to channel gating, results in little structural alteration of the transmembrane domain.

As noted, the main change in structure in the nAChR upon desensitization may be a closing of the C-loop of the ligand-binding domain, as is observed upon the binding of ligands to the acetylcholine-binding protein (18). This would account for the high affinity of the nAChR for Carb in the desensitized state. The structure of the transmembrane domain of the nAChR in the desensitized state may be very similar to the structure of the transmembrane domain in the resting state. Ligand binding, however, must be uncoupled from channel activation. Recent studies of *cys*-loop receptor channel gating have identified the structural interface between the transmembrane and ligand-binding domains (34–36). The uncoupling of ligand binding and channel activation may very well occur at this structural interface.

Finally, our data show that the vibration centered near 1720 cm^{-1} in the Carb-difference spectra, which is due primarily to the ester carbonyl stretch of the nAChR bound Carb, is more intense in Carb-difference spectra recorded using infrared light polarized in the perpendicular versus parallel orientation direction, suggesting that the carbonyl group has a preferential orientation perpendicular to the bilayer normal. In the crystal structure of Carb bound to the acetylcholine binding protein, the ester carbonyl is placed in the electron density so that the C=O is oriented close to parallel to the bilayer normal while the C-NH_2 bond is orientated close to perpendicular (5). Our results suggests that the carbonyl oxygen and adjacent –NH_2 group of Carb should be reversed in the crystal structure.

CONCLUSIONS

Linear dichroism FTIR spectra show that the exchange-resistant α-helical peptides in the nAChR are oriented preferentially perpendicular to the bilayer surface. No net changes in the orientation of transmembrane α-helices can be detected upon agonist binding and desensitization. In fact, the main changes in structure/orientation of the peptide backbone upon desensitization appear to involve regions of the peptide backbone that are highly accessible to solvent. Desensitization of the nAChR may result from a capping of the ligand-binding site by the solvent-accessible C-loop, with little change in structure of the transmembrane domain. The structural change that uncouples ligand binding to the nAChR from channel gating in the desensitized state remains to be defined.

SUPPLEMENTARY MATERIAL

An online supplement to this article can be found by visiting BJ Online at http://www.biophysj.org.

This work was supported by grants from the Canadian Institutes of Health Research to J.E.B. and a Natural Sciences and Engineering Research Council of Canada graduate scholarship to D.G.H.

REFERENCES

1. Karlin, A. 2002. Emerging structure of the nicotinic acetylcholine receptors. *Nat. Rev. Neurosci.* 3:102–114.
2. Unwin, N. 2003. Structure and action of the nicotinic acetylcholine receptor explored by electron microscopy. *FEBS Lett.* 555:91–95.
3. Lester, H. A., M. I. Dibas, D. S. Dahan, J. F. Leite, and D. A. Dougherty. 2004. *Cys*-loop receptors: new twists and turns. *Trends Neurosci.* 27:329–336.
4. Brejc, K., W. J. van Dijk, R. V. Klaassen, M. Schuurmans, J. van Der Oost, A. B. Smit, and T. K. Sixma. 2001. Crystal structure of an AChbinding protein reveals the ligand-binding domain of nicotinic receptors. *Nature.* 411:269–276.
5. Celie, P. H., S. E. van Rossum-Fikkert, W. J. van Dijk, K. Brejc, A. B. Smit, and T. K. Sixma. 2004. Nicotine and carbamylcholine binding to nicotinic acetylcholine receptors as studied in AChBP crystal structures. *Neuron.* 41:907–914.
6. Unwin, N. 1993. Nicotinic acetylcholine receptor at 9 Å resolution. *J. Mol. Biol.* 229:1101–1124.
7. Görne-Tschelnokow, U., A. Strecker, C. Kaduk, D. Naumann, and F. Hucho. 1994. The transmembrane domains of the nicotinic acetylcholine receptor contain α-helical and β structures. *EMBO J.* 13:338–341.
8. Noda, M., H. Takahashi, T. Tanabe, M. Toyosato, S. Kikyotani, Y. Furutani, T. Hirose, H. Takashima, S. Inayama, T. Miyata, and S. Numa. 1983. Structural homology of *Torpedo californica* acetylcholine receptor subunits. *Nature.* 302:528–532.
9. Blanton, M. P., and J. B. Cohen. 1992. Mapping the lipid-exposed regions in the *Torpedo californica* nicotinic acetylcholine receptor. *Biochemistry.* 31:3738–3750.
10. Blanton, M. P., and J. B. Cohen. 1994. Identifying the lipid-protein interface of the *Torpedo* nicotinic acetylcholine receptor: secondary structure implications. *Biochemistry.* 33:2859–2872.
11. Méthot, N., and J. E. Baenziger. 1998. Secondary structure of the exchange-resistant core from the nicotinic acetylcholine receptor probed directly by infrared spectroscopy and hydrogen/deuterium exchange. *Biochemistry.* 37:14815–14822.
12. Méthot, N., B. D. Ritchie, M. P. Blanton, and J. E. Baenziger. 2001. Structure of the pore-forming transmembrane domain of a ligand-gated ion channel. *J. Biol. Chem.* 276:23726–23732.
13. Corbin, J., N. Méthot, H. H. Wang, J. E. Baenziger, and M. P. Blanton. 1998. Secondary structure analysis of individual transmembrane segments of the nicotinic acetylcholine receptor by circular dichroism and Fourier transform infrared spectroscopy. *J. Biol. Chem.* 273:771–777.
14. Opella, S. J., F. M. Marassi, J. J. Gesell, A. P. Valente, Y. Kim, M. Oblatt-Montal, and M. Montal. 1999. Structures of the M2 channel-lining segments from nicotinic acetylcholine and NMDA receptors by NMR spectroscopy. *Nat. Struct. Biol.* 6:374–379.
15. Miyazawa, A., Y. Fujiyoshi, and N. Unwin. 2003. Structure and gating mechanism of the acetylcholine receptor pore. *Nature.* 423:949–955.
16. Unwin, N. 2005. Refined structure of the nicotinic acetylcholine receptor at 4 Å resolution. *J. Mol. Biol.* 346:967–989.
17. Unwin, N. 1995. Acetylcholine receptor channel imaged in the open state. *Nature.* 373:37–43.
18. Hansen, S. B., G. Sulzenbacher, T. Huxford, P. Marchot, P. Taylor, and Y. Bourne. 2005. Structures of *Aplysia* AChBP complexes with nicotinic agonists and antagonists reveal distinctive binding interfaces and conformations. *EMBO J.* 24:3635–3646.
19. Lee, W. Y., and S. M. Sine. 2005. Principal pathway coupling agonist binding to channel gating in nicotinic receptors. *Nature.* 438:243–247.
20. Lummis, S. C., D. L. Beene, L. W. Lee, H. A. Lester, R. W. Broadhurst, and D. A. Dougherty. 2005. *Cis-trans* isomerization at a proline opens the pore of a neurotransmitter-gated ion channel. *Nature.* 438:248–252.
21. Xiu, X., A. P. Hanek, J. Wang, H. A. Lester, and D. A. Dougherty. 2005. A unified view of the role of electrostatic interactions in modulating the gating of Cys loop receptors. *J. Biol. Chem.* 280:41655–41666.
22. Grutter, T., L. P. de Carvalho, V. Dufresne, A. Taly, S. J. Edelstein, and J. P. Changeux. 2005. Molecular tuning of fast gating in pentameric ligand-gated ion channels. *Proc. Natl. Acad. Sci. USA.* 102:18207–18212.
23. daCosta, C. J. B., A. A. Ogrel, E. A. McCardy, M. P. Blanton, and J. E. Baenziger. 2002. Lipid-protein interactions at the nicotinic acetylcholine receptor. A functional coupling between nicotinic receptors and phosphatidic acid-containing lipid bilayers. *J. Biol. Chem.* 277:201–208.
24. Griffiths, P., and G. L. Pariente. 1986. Introduction to spectral deconvolution. *Trends Analyt. Chem.* 5:209–215.
25. Baenziger, J. E., K. W. Miller, and K. J. Rothschild. 1992. Incorporation of the nicotinic acetylcholine receptor into planar multilamellar films: characterization by fluorescence and Fourier transform infrared difference spectroscopy. *Biophys. J.* 61:983–992.
26. Hübner, W., and H. H. Mantsch. 1991. Orientation of specifically $^{13}C{=}O$ labeled phosphatidylcholine multilayers from polarized attenuated total reflection FT-IR spectroscopy. *Biophys. J.* 59:1261–1272.
27. Goormaghtigh, E., and J. M. Ruysschaert. 1990. Polarized attenuated total reflection infrared spectroscopy as a tool to investigate the conformation and orientation of membrane components. *In* Molecular Description of Biological Membranes by Computer Aided Conformational Analysis. R. Brasseur, editor. CRC Press, Boca Raton, FL. 285–329.
28. Rothschild, K. J., and N. A. Clark. 1979. Polarized infrared spectroscopy of oriented purple membrane. *Biophys. J.* 25:473–487.
29. Bradbury, E. M., L. Brown, A. R. Downie, A. Elliott, R. D. Fraser, and W. E. Hanby. 1962. The structure of the ω-form of poly-β-benzyl-L-aspartate. *J. Mol. Biol.* 5:230–247.
30. Tsuboi, M. 1962. Infrared dichroism and molecular conformation of α-form poly-γ-benzyl-L-glutamate. *J. Polym. Sci. [B].* 59:139–153.
31. Marsh, D., M. Muller, and F. J. Schmitt. 2000. Orientation of the infrared transition moments for an α-helix. *Biophys. J.* 78:2499–2510.
32. Fong, T. M., and M. G. McNamee. 1986. Correlation between acetylcholine receptor function and structural properties of membranes. *Biochemistry.* 25:830–840.
33. McCarthy, M. P., and M. A. Moore. 1992. Effects of lipids and detergents on the conformation of the nicotinic acetylcholine receptor from *Torpedo californica*. *J. Biol. Chem.* 267:7655–7663.
34. Ryan, S. E., C. N. Demers, J. P. Chew, and J. E. Baenziger. 1996. Structural effects of neutral and anionic lipids on the nicotinic acetylcholine receptor. An infrared difference spectroscopy study. *J. Biol. Chem.* 271:24590–24597.
35. DeLange, F., P. H. Bovee-Geurts, A. M. Pistorius, K. J. Rothschild, and W. J. DeGrip. 1999. Probing intramolecular orientations in rhodopsin and metarhodopsin II by polarized infrared difference spectroscopy. *Biochemistry.* 38:13200–13209.
36. Gonen, T., Y. Cheng, P. Sliz, Y. Hiroaki, Y. Fujiyoshi, S. C. Harrison, and T. Walz. 2005. Lipid-protein interactions in double-layered two-dimensional AQP0 crystals. *Nature.* 438:633–638.
37. Baenziger, J. E., and N. Méthot. 1995. Fourier transform infrared and hydrogen/deuterium exchange reveal an exchange-resistant core of α-helical peptide hydrogens in the nicotinic acetylcholine receptor. *J. Biol. Chem.* 270:29129–29137.
38. Baenziger, J. E., and J. P. Chew. 1997. Desensitization of the nicotinic acetylcholine receptor mainly involves a structural change in solvent-accessible regions of the polypeptide backbone. *Biochemistry.* 36: 3617–3624.
39. Ryan, S. E., D. G. Hill, and J. E. Baenziger. 2002. Dissecting the chemistry of nicotinic receptor-ligand interactions with infrared difference spectroscopy. *J. Biol. Chem.* 277:10420–10426.